ORIGINAL ARTICLE

COL4A1 Mutations and Hereditary Angiopathy, Nephropathy, Aneurysms, and Muscle Cramps

Emmanuelle Plaisier, M.D., Olivier Gribouval, M.Sc., Sonia Alamowitch, M.D., Béatrice Mougenot, M.D., Catherine Prost, M.D., Marie Christine Verpont, M.Sc., Béatrice Marro, M.D., Thomas Desmettre, M.D., Salomon Yves Cohen, M.D., Etienne Roullet, M.D.,* Michel Dracon, M.D., Michel Fardeau, M.D., Tom Van Agtmael, Ph.D., Dontscho Kerjaschki, M.D., Corinne Antignac, M.D., and Pierre Ronco, M.D.

ABSTRACT

BACKGROUND

COL4A3, *COL4A4*, and *COL4A5* are the only collagen genes that have been implicated in inherited nephropathies in humans. However, the causative genes for a number of hereditary multicystic kidney diseases, myopathies with cramps, and heritable intracranial aneurysms remain unknown.

METHODS

We characterized the renal and extrarenal phenotypes of subjects from three families who had an autosomal dominant hereditary angiopathy with nephropathy, aneurysms, and muscle cramps (HANAC), which we propose is a syndrome. Linkage studies involving microsatellite markers flanking the *COL4A1–COL4A2* locus were performed, followed by sequence analysis of *COL4A1* complementary DNA extracted from skin-fibroblast specimens from the subjects.

RESULTS

We identified three closely located glycine mutations in exons 24 and 25 of the gene *COL4A1*, which encodes procollagen type IV α1. The clinical renal manifestations of the HANAC syndrome in these families include hematuria and bilateral, large cysts. Histologic analysis revealed complex basement-membrane defects in kidney and skin. The systemic angiopathy of the HANAC syndrome appears to affect both small vessels and large arteries.

CONCLUSIONS

COL4A1 may be a candidate gene in unexplained familial syndromes with autosomal dominant hematuria, cystic kidney disease, intracranial aneurysms, and muscle cramps.

From INSERM Unité 702 (E.P., B. Mougenot, M.C.V., P.R.); Université Pierre et Marie Curie, Paris 6, Unités Mixtes de Recherche Scientifique 702 (E.P., M.C.V., P.R.) and 582 (M.F.); Assistance Publique–Hôpitaux de Paris, Hôpital Tenon (E.P., S.A., B. Marro, E.R., P.R.), Hôpital Avicenne (C.P.), Hôpital Pitié–Salpêtrière (M.F.), and Hôpital Necker (C.A.); INSERM Unité 574 (O.G., C.A.); Center of Ophthalmology, Paris 15 (S.Y.C.); INSERM Unité 582 (M.F.); and Université Paris Descartes, Faculté de Médecine René Descartes, Unité Mixte de Recherche Scientifique 574 (C.A.) — all in Paris; Université Lille 2 (T.D.) and Centre Hospitalier Régional Universitaire Lille (M.D.) — both in Lille, France; University of Edinburgh, Queens Medical Research Institute, Edinburgh (T.V.A.); and Medical University of Vienna, Clinical Institute of Pathology, Vienna (D.K.). Address reprint requests to Dr. Plaisier at the Department of Nephrology and INSERM Unité 702, Hôpital Tenon, 4 Rue de la Chine, 75020 Paris, France, or at emmanuelle.plaisier@tnn.aphp.fr.

*Dr. Roullet is deceased.

N Engl J Med 2007;357:2687-95.

Six alpha chains of type IV collagen — α1(IV) through α6(IV) — produce three networks of type IV collagen: α1.α1.α2(IV), α3.α4.α5(IV), and α5.α5.α6(IV). These three networks are the main component of basement membranes. Alpha chains of type IV collagen consist of an N-terminal 7S domain; a triple-helical collagenous domain, containing the classic Gly–Xaa–Yaa repeat amino acid sequence; and a C-terminal noncollagenous NC1 domain.[1] The α1.α1.α2(IV) network is widely expressed in the body, whereas the α3.α4.α5(IV) and α5.α5.α6(IV) networks have a tissue-restricted expression. In the kidney, the α3.α4.α5(IV) network replaces the α1.α1.α2(IV) network during embryogenesis of the glomerular basement membrane, whereas the basement membrane of tubules and Bowman's capsules are composed mainly of a mixed α1.α1.α2(IV)–α5.α5.α6(IV) network.[2]

Alport's syndrome is caused by mutations in type IV collagen. The most common X-linked form is caused by mutations in *COL4A5* (Online Mendelian Inheritance in Man [OMIM] number 301050), but 15% of cases of Alport's syndrome are due to autosomal recessive (or in rare cases, dominant) mutations affecting either *COL4A3* or *COL4A4* (OMIM numbers 203780 and 104200, respectively).[1] The clinical phenotype of Alport's syndrome correlates with the expression pattern of α3.α4.α5(IV). In addition, 50% of cases of familial benign hematuria have been attributed to mutations in *COL4A3* or *COL4A4*.[1]

Mutations in *COL4A1* have recently been identified in both a mouse model and families with porencephaly, a rare autosomal dominant condition characterized by cystic brain cavities and cerebral white-matter lesions.[3-6] *COL4A1* mutations have also been found in a single family with small-vessel disease affecting the brain and the eye.[6,7]

The widespread expression of the α1.α1.α2(IV) network suggests that *COL4A1* mutations may lead to a systemic phenotype. We describe *COL4A1* mutations in subjects from three families who have hereditary angiopathy with nephropathy, aneurysms, and muscle cramps, which we call the HANAC syndrome. The nephropathy consisted of persistent hematuria or bilateral, large cysts. The angiopathy affects both small vessels and large arteries and causes leukoencephalopathy, retinal arteriolar tortuosity, and intracranial aneurysms. All three *COL4A1* mutations, localized in exons 24 and 25, affect glycine residues, interrupting the Gly–Xaa–Yaa amino acid repeat.

METHODS

CLINICAL EVALUATION

Written informed consent was obtained from all subjects or their parents. Phenotypic studies included clinical evaluation, urinalysis, measurement of serum creatinine levels and urinary protein excretion, estimation of the glomerular filtration rate with the use of the four-variable Modification of Diet in Renal Disease equation,[8] abdominal ultrasonic tomography, abdominal computed tomography (CT) or renal magnetic resonance imaging (MRI), muscle testing and measurement of serum creatine kinase levels, funduscopic examination and fluorescein angiography, brain MRI, and cerebral magnetic resonance angiography or CT angiography.

GENETIC-LINKAGE ANALYSIS

Genomic DNA was extracted according to standard methods. For haplotype analyses, we used polymorphic microsatellite markers — D13S173, D13S126, D13S1315, and D13S261 — that span the genetic interval of the *COL4A1–COL4A2* locus at 13q34.

DETECTION OF MUTATIONS

Primary fibroblasts were cultured from skin-biopsy specimens. Total RNA was isolated from the cultured fibroblasts with RNAwiz (Ambion). Complementary DNA (cDNA) was synthesized with the use of the Superscript first-strand synthesis system for the reverse-transcriptase–polymerase-chain-reaction assay (Invitrogen). Full-length *COL4A1* cDNA was amplified with the use of 11 primer pairs, and both strands were sequenced. Family members and 150 ethnically matched controls were screened for mutations with the use of specific primers amplifying *COL4A1* exon 24 or exon 25. (The sequences of all primers are listed in the Supplementary Appendix, available with the full text of this article at www.nejm.org.)

ELECTRON MICROSCOPY AND IMMUNOGOLD ELECTRON MICROSCOPY

Electron microscopy was performed as previously described.[9] Immunogold electron microscopy was

performed on ultrathin frozen sections of kidney-biopsy specimens as previously described.[10] Sections were processed for indirect immunogold labeling with the use of rabbit antihuman α1(IV) and α2(IV) antibodies (dilution, 1:120) (Novotec).

RESULTS

PHENOTYPIC EVALUATION

The phenotypic characteristics of affected subjects are shown in Figure 1 and listed in Table 1.

Family 1

In Family 1, the clinical phenotype was transmitted as an autosomal dominant trait (Fig. 2A).[9] All affected subjects presented with microscopic hematuria, muscle cramps with elevated creatine kinase levels, and bilateral retinal arteriolar tortuosity that caused repeated retinal hemorrhages (Fig. 1J). Gross hematuria occurred in Subjects III-1, III-3, and IV-4; supraventricular cardiac arrhythmia occurred in Subjects II-2, III-1, and IV-1; and Raynaud's phenomenon occurred in Subjects III-1, III-3, IV-1, IV-2, and IV-4. All affected subjects had normal blood pressure.

Renal CT revealed small, bilateral cysts in Subjects II-2, III-1, and III-3. Brain MRI revealed white-matter abnormalities and dilated microvascular spaces in Subjects III-1, III-3, IV-2, and IV-4 (Fig. 1D). Aneurysms affected the intracranial segment of the right internal carotid artery in Subjects III-3 (Fig. 1G), IV-2 (aneurysm diameter, 6 mm), and IV-4 (aneurysm diameter, 4 mm), and an aneurysm, 2 mm in diameter, was detected in the horizontal segment of the right middle cerebral artery in Subject IV-4. The results of cerebral imaging were normal for Subject IV-1 and were not available for Subject III-5. Subject III-3, who was 48 years of age at the time of imaging, had previously had a lacunar infarct of the brain stem.

Subjects IV-1 and IV-4 underwent kidney biopsy because of persistent microscopic hematuria. The tissue sections showed no abnormalities on light microscopy (Fig. 1A, top), and immunofluoresence studies showed normal expression of COL4A1 (Fig. 1S, Panels C and D, in the Supplementary Appendix) and of COL4A3 and COL4A5 (reported previously[9] for Subject IV-1 and not shown for Subject IV-4). The expression of laminin α5 and perlecan was normal (Fig. 2S, Panels A and B, in the Supplementary Appendix), but there was no apparent induction of laminin-5 and integrin β_4 in the tubular basement membrane (data not shown). Electron-microscopical examination of the kidney-biopsy specimens from Subjects IV-1 and IV-4 revealed similar alterations of the basement membranes of the Bowman's capsule, tubules, and interstitial capillaries (Fig. 1A and Fig. 3A, 3B, 3C, 3D, and 3E). These alterations were characterized by irregular thickening, splitting in multiple layers, and electron-lucent areas. Numerous focal interruptions of the basement membrane were seen in interstitial capillaries (Fig. 3A). In contrast, the glomerular basement membrane had a normal appearance and thickness (Fig. 1S, Panels A and B, in the Supplementary Appendix).[9] Immunoelectron microscopy showed normal expression of α1.α1.α2(IV) trimers in the glomerular basement membrane (Fig. 1S, Panel E, in the Supplementary Appendix) and in the tubular and interstitial capillary basement membranes, except in electron-lucent areas (Fig. 3G).

Similar alterations of the basement membrane, including duplications, were seen in the skin at the dermoepidermal junction in Subjects III-3 and IV-4 (Fig. 4A and 4B). In dermal arterioles, vascular smooth-muscle cells were dissociated, with abnormal spreading of the basement membrane (Fig. 4E and 4F). The muscle ultrastructure was normal.

Family 2

In Family 2, the affected subjects (Fig. 2A) presented with bilateral retinal arteriolar tortuosity, which caused hemorrhages in Subjects I-1, II-1, and II-3 (Fig. 1K). Clinical evaluations and genetic studies were performed in Subject II-1 and in his two daughters (25-year-old Subject III-1 and 21-year-old Subject III-2). Subject II-1 had mild renal failure (glomerular filtration rate, 56 ml per minute per 1.73 m^2 of body-surface area), without proteinuria or hematuria, normal blood pressure, and bilateral large cysts (Fig. 1B). The size of the left kidney was normal (long-axis length, 113 mm), but the lower pole of the right kidney (long-axis length, 138 mm) was deformed by a massive cyst (90 mm in diameter). Subject II-1 also had periventricular white-matter abnormalities (Fig. 1E). Subject III-2 had neither renal abnormalies nor a brain lesion, but she did have elevated creatine kinase levels, without muscle cramps, and an an-

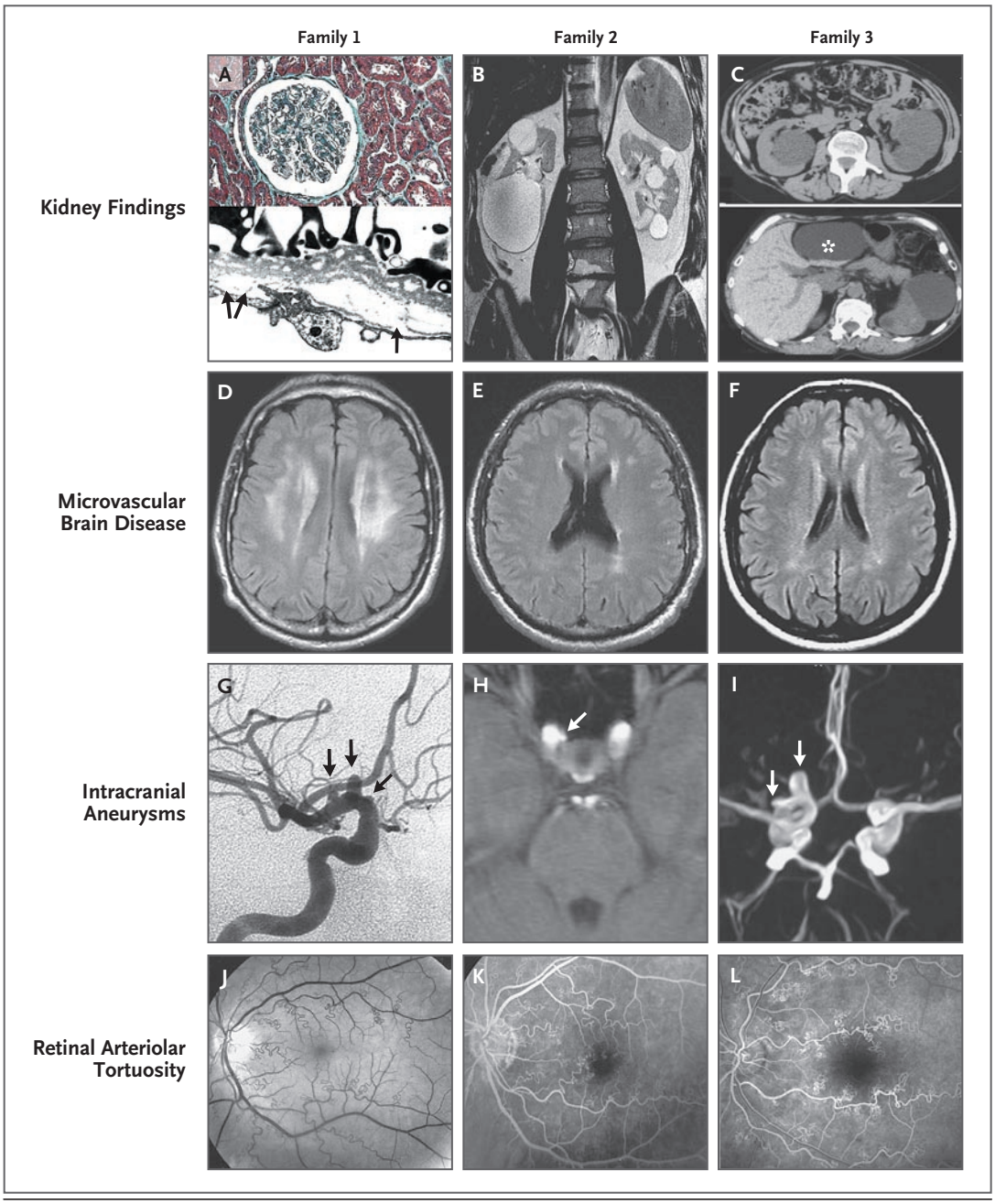

eurysm of the right internal carotid artery, 2 mm in diameter (Fig. 1H). Funduscopic, renal, and cerebral evaluations in Subject III-1 were normal.

Family 3

In Family 3, retinal arteriolar tortuosity and hemorrhages were found in Subjects I-1 and II-3 (Fig. 1L and 2A). Data from detailed investigations were available for Subject II-3, in whom muscle cramps that limited exercise developed during childhood. The serum creatine kinase level was persistently elevated, and electromyograms were normal. Renal evaluations revealed mild renal failure (glomerular filtration rate, 52 ml per minute per 1.73 m^2) — without hypertension, proteinuria, or hematuria — and bilateral, large cysts, the largest of which was 140 by 84 mm and was in the left kidney (Fig. 1C). A large hepatic cyst

Figure 1 (facing page). Phenotypic Characterization of Patients with the Hereditary Angiopathy with Nephropathy, Aneurysms, and Muscle Cramps (HANAC) Syndrome.

Kidney-tissue specimens from Subject IV-1, Family 1, were normal on light microscopy (Panel A, top; Masson stain), but electron microscopy (Panel A, bottom) revealed marked thickening of the tubular basement membrane, with electron-lucent areas, associated with focal disruptions of the interstitial capillary basement membrane (arrows). Large, bilateral renal cysts were visible in the cortex and the medulla on magnetic resonance imaging (MRI) in Subject II-1, Family 2 (Panel B), and on computed tomography (CT) of the abdomen in Subject II-3, Family 3 (who also had a liver cyst [asterisk]) (Panel C). Cerebral MRI with fluid-attenuated inversion recovery sequences showed periventricular leukoencephalopathy in Subject III-3, Family 1 (Panel D); in Subject II-1, Family 2 (Panel E); and in Subject II-3, Family 3 (Panel F). Aneurysms were found in the intracranial portion of the right internal carotid artery on cerebral angiography in Subject III-3, Family 1 (Panel G, arrows [from left to right, 2 mm, 3 mm, and 1.5 mm in diameter, respectively]); on magnetic resonance angiography in Subject III-2, Family 2 (Panel H, arrow [2 mm in diameter]); and on CT angiography in Subject II-3, Family 3 (Panel I, arrows [from left to right, 6 mm and 8 mm in diameter, respectively]). In Panels J, K, and L, representative fluorescein angiograms show bilateral, posterior retinal arteriolar tortuosity.

(91 by 65 mm) was also detected (Fig. 1C). Fifteen years earlier, ultrasonography had revealed smaller cysts in the left kidney (50 mm in diameter) and in the liver (40 mm in diameter). Subject II-3 had posterior leukoencephalopathy (Fig. 1F) and three aneurysms (2, 6, and 8 mm in diameter) in the right internal carotid artery, Raynaud's phenomenon, and paroxysmal supraventricular cardiac arrhythmia. Funduscopic, renal, and cerebral evaluations were normal in Subjects II-1 and III-2.

A skin biopsy was performed in Subjects II-3 (with the *COL4A1* mutation) and III-2 (without the mutation) to determine whether a skin-membrane disease (basalopathy) was present. Subject II-3 had alterations of the basement membrane at the dermoepidermal junction and in vessel walls (Fig. 4C and 4G), which were similar to those seen in Subjects III-3 (Fig. 4A and 4E) and IV-4 (Fig. 4B and 4F) in Family 1. The ultrastructure of the skin was normal in Subject III-2 (Fig. 4D and 4H).

GENETIC ANALYSES

Linkage analysis indicated that all affected subjects in Family 1 shared a common haplotype at the *COL4A1–COL4A2* locus (data not shown). Sequence analysis of *COL4A1* cDNA from Subject IV-1 revealed the heterozygous missense mutation c.1493G→T in exon 24, responsible for a glycine-to-valine substitution (p.Gly498→Val) (Fig. 2A). This mutation was present in all affected subjects in Family 1 who were alive. Subjects II-1 and III-2 from Family 2 had the missense mutation c.1555G→A in exon 25, leading to a glycine-to-arginine substitution (p.Gly519→Arg) (Fig. 2A). In Family 3, the missense mutation c.1583G→A was detected in exon 25, leading to the substitution of glutamic acid for glycine (p.Gly528→Glu) (Fig. 2A). No mutations were found in the 150

Table 1. Clinical Characteristics of Families with the Hereditary Angiopathy with Nephropathy, Aneurysms, and Muscle Cramps (HANAC) Syndrome.

Characteristic	Family 1	Family 2	Family 3
Race*	White	White	White
Kidney	Isolated hematuria, normal glomerular filtration rate	Bilateral cysts, decreased glomerular filtration rate	Bilateral cysts, decreased glomerular filtration rate
Muscle	Cramps, elevated creatine kinase levels	Asymptomatic, elevated creatine kinase levels	Cramps, elevated creatine kinase levels
Intracranial vessels	Multiple aneurysms of the right internal carotid artery, single aneurysm of the middle cerebral artery	Single aneurysm of the right internal carotid artery	Multiple aneurysms of the right internal carotid artery
Results of brain MRI	Leukoencephalopathy	Leukoencephalopathy	Leukoencephalopathy
Retinal vessels	Retinal arteriolar tortuosity	Retinal arteriolar tortuosity	Retinal arteriolar tortuosity
Other	Raynaud's phenomenon, cardiac arrhythmia		Raynaud's phenomenon, cardiac arrhythmia

* Race was self-reported.

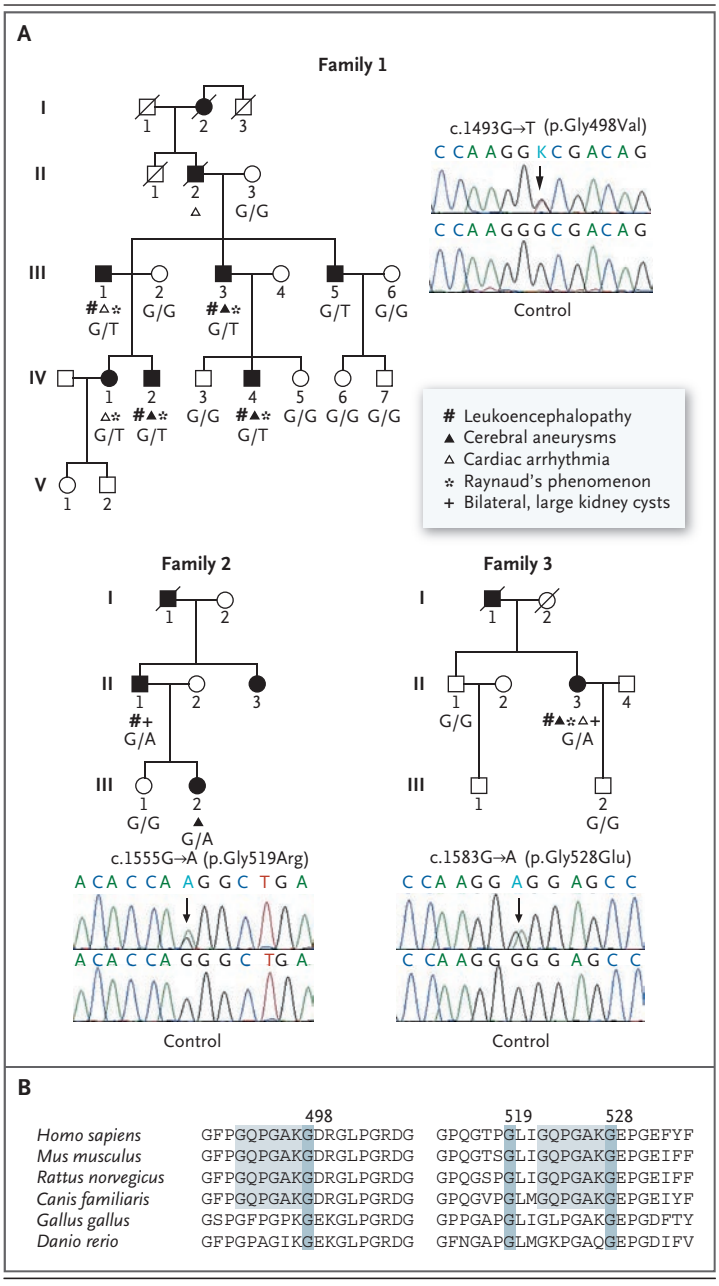

Figure 2. Pedigrees and *COL4A1* Mutations of Families 1, 2, and 3.

In the pedigree for Family 1 (Panel A, left), black squares and circles indicate affected male and female subjects, respectively, presenting with hematuria, muscle cramps, and retinal arterial tortuosity; electrophoregrams from an affected subject (top, with "K" denoting G–T heterozygosity) and a control (bottom) are also shown. All affected subjects had the heterozygous missense mutation c.1493G→T in *COL4A1* exon 24, leading to a change from glycine to valine at position 498. In the pedigree for Family 2, black squares and circles indicate male and female subjects, respectively, presenting with retinal arterial tortuosity. Electrophoregrams below the pedigree show a heterozygous c.1555G→A transition in *COL4A1* exon 25 in an affected subject, resulting in a change from glycine to arginine at position 519. In the pedigree for Family 3, black squares and circles indicate male and female subjects, respectively, presenting with retinal arterial tortuosity and retinal hemorrhage. Electrophoregrams below the pedigree show the heterozygous missense mutation c.1583G→A in *COL4A1* exon 25 in an affected subject, leading to a change from glycine to glutamic acid at position 528. In Panel A, a slash over a symbol denotes death, markers below the symbols denote additional phenotypic characteristics of the affected subjects, and uppercase letters denote the *COL4A1* alleles. Panel B shows the evolutionary conservation of the Gly498, Gly519, and Gly528 residues among species. The Gly498 and Gly528 residues are both localized at the C-terminal end of an identical sequence of seven amino acids (blue shading). Amino acids are represented with their single-letter symbols.

ethnically similar control samples (representing 300 chromosomes). The three affected glycine residues are located near one another in the collagenous domain, at sites that are highly conserved (Fig. 2B). The Gly498 and Gly528 residues are located at the C-terminal end of an identical amino acid sequence (Gly–Glu–Pro–Gly–Ala–Lys–Gly). This sequence is not present in other segments of the COL4A1 protein and is conserved among vertebrate species (Fig. 2B).

DISCUSSION

We have identified three mutations of the *COL4A1* gene that appear to be associated with a systemic disease we call the HANAC syndrome. All three mutations affect glycine residues that are close to each other, located in exons 24 and 25, suggesting that these exons may encode critical functional domains of the COL4A1 triple helix.

The identification of *COL4A1* mutations in patients with the HANAC syndrome extends the spectrum of diseases associated with heterozygous *COL4A1* mutations. Previously reported mutations are associated with dominant small-vessel disease affecting only retinal vessels and the brain.[3-6] In contrast, the HANAC syndrome affects the kidney, muscle, and cardiovascular system, including retinal and cerebral vessels. Moreover, the condition affects large vessels (through intracranial aneurysms). The HANAC syndrome is phenotypically distinct from hereditary endo-

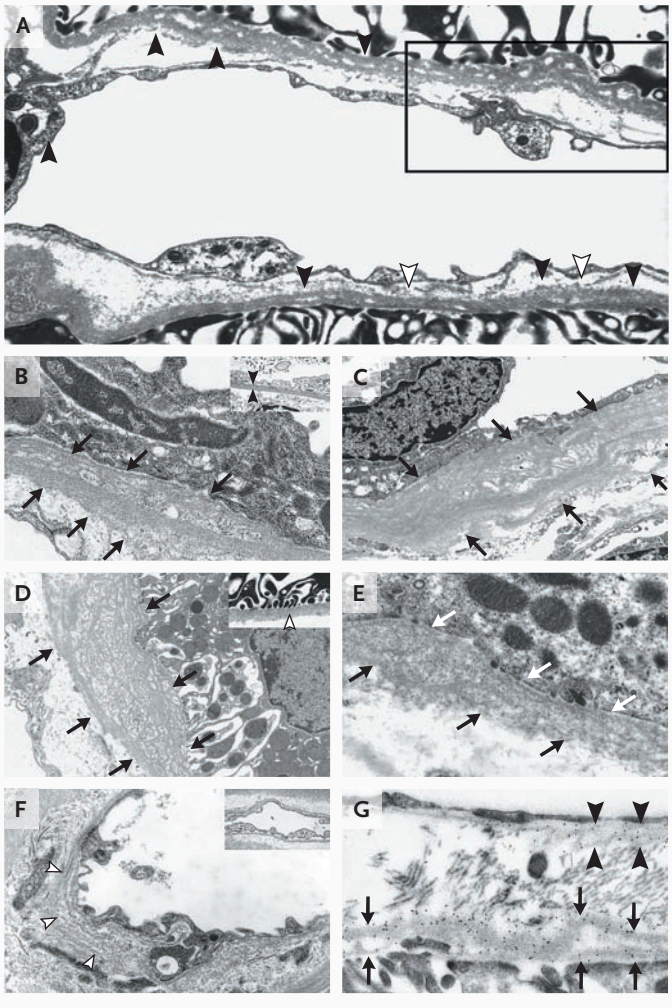

Figure 3. Abnormalities of the Renal Basement Membrane in Subjects IV-1 and IV-4, Family 1.

A low-magnification electron micrograph of a kidney specimen from Subject IV-1 (Panel A) shows a longitudinal section of an interstitial capillary with adjacent tubules, demonstrating diffuse alterations in the basement membrane. The inset in Panel A is also shown in Figure 1A as part of the phenotypic characterization of the hereditary angiopathy with nephropathy, aneurysms, and muscle cramps syndrome. There is irregular thickening of the tubule basement membrane, which contains multiple electron-lucent areas (black arrowheads) and focal disruptions of the interstitial capillary basement membrane (white arrowheads). In several areas, the interstitial capillary basement membrane is fuzzy and detached from the underlying endothelial cells. Electron micrographs of the basement membrane in the Bowman's capsule (Panel B, Subject IV-4, and Panel C, Subject IV-1) and the tubule (Panel D, Subject IV-4, and Panel E, Subject IV-1) show thickening and splitting with multiple laminations and electron-lucent areas (the arrows show the basement membrane). The tubular basement membrane has an appearance reminiscent of the "basket-weave" aspect of the glomerular basement membrane in Alport's syndrome. The basement membrane of interstitial capillaries in Subject IV-4 shows a large area of lamination (Panel F, white arrowheads). The insets in Panels B and D (arrowheads) and in Panel F show normal basement membranes from a control subject with thin-basement-membrane nephropathy. Panel G shows normal expression of the $\alpha 1.\alpha 1.\alpha 2$(IV) trimer in duplicated tubular basement membrane (arrows) and along basement membrane of the interstitial capillaries, as revealed by immunogold electron microscopy of a specimen from Subject IV-4. The interstitial capillary basement membrane also shows areas of duplication (arrowheads). These abnormalities were observed in both affected subjects, even though their kidney specimens had a completely normal appearance on light microscopy.

theliopathy with retinopathy, nephropathy, and stroke, which maps to chromosome 3p21.[11]

In Family 1, hematuria was consistently associated with the other manifestations of the HANAC syndrome. Severe ultrastructural defects of the basement membrane in Bowman's capsules, tubules, and interstitial capillaries were detected in both affected subjects studied. Similar alterations were observed in skin basement membrane; together with the clinical phenotype, this finding points to widespread basement-membrane disease. Mice that have *Col4a1* mutations such as those related to bruising at birth (*Col4a1*$^{+/Bru}$) or to retinal arteriolar wiring (*Col4a1*$^{+/Raw}$) also have focal basement-membrane disruptions in multiple tissues and splitting of the basement membrane of the Bowman's capsule.[12] In contrast, the glomerular basement membrane has a normal appearance in patients with the HANAC syndrome, in *Col4a1*$^{+/Bru}$ mice, and in *Col4a1*$^{+/Raw}$ mice. These findings can be explained by the predominance in adults of the $\alpha 1.\alpha 1.\alpha 2$(IV) trimer in most basement membranes, except for that of the glomerulus. The anomalies of the tubular basement membrane are reminiscent of the "basket-weave" appearance of the glomerular basement membrane in patients with Alport's syndrome. We hypothesize that the hematuria seen in Family 1 may be the result of defects in the basement membrane of the tubules and the peritubular capillaries.

In Families 2 and 3, the phenotype was char-

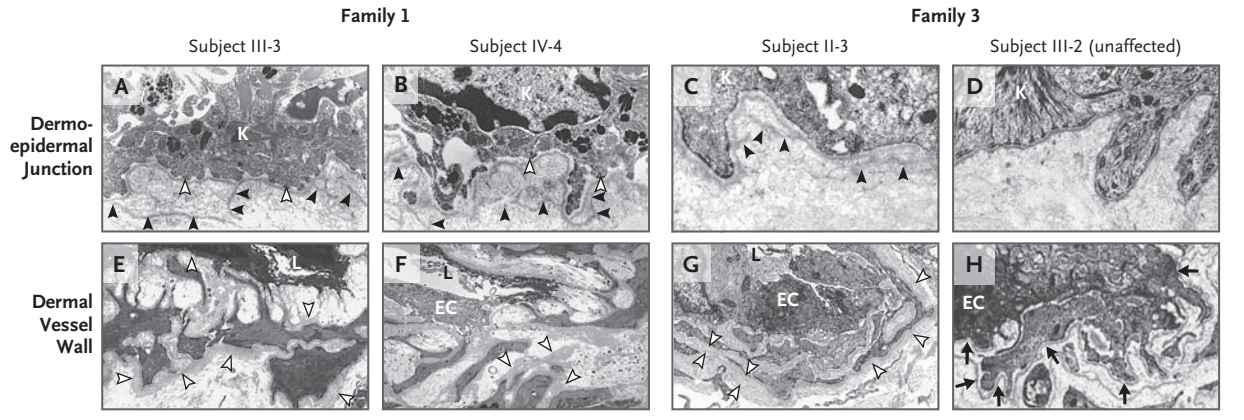

Figure 4. Abnormalities of the Skin Basement Membrane in Families 1 and 3.

In Panels A, B, and C, electron micrographs of the dermoepidermal junction show replication of the lamina densa (black arrowheads), with normal hemidesmosomes (white arrowheads), in affected subjects. In Panel D, the lamina densa in Subject III-2, Family 3, is normal. In Panels E, F, and G, electron micrographs of dermal arterioles show substantial expansion and thickening of the lamina densa (white arrowheads), between smooth-muscle cells. The basement membrane in the vessel wall is of normal thickness in Subject III-2, Family 3 (Panel H, arrows). These abnormalities were found in subjects whose skin had a completely normal appearance on physical examination and light microscopy. K denotes keratinocytes, EC endothelial cells, and L arteriole lumen.

acterized by bilateral renal cysts and mild renal failure. The cysts in the renal poles were very large, although the overall size of the kidney remained roughly preserved. The absence of renal cysts in Subject III-2 in Family 2, who was 20 years old, might be related to the development of cysts with age. Small bilateral cysts were also found in older members of Family 1. The cystic phenotype is different from that in polycystic kidney diseases or medullary cystic kidney disease. Cyst formation is usually associated with abnormal remodeling of the extracellular matrix and altered composition of the basement membrane.[13,14] Kidney biopsy was not performed in affected subjects from Families 2 and 3 because of the presence of cysts. However, a skin-biopsy specimen from Subject II-3 in Family 3 showed basement-membrane alterations similar to those in affected subjects in Family 1. These findings, together with the previously reported association of a hypomorphic mutation in the laminin $\alpha 5$ gene with polycystic kidney disease,[15] indicate the importance of components of the basement membrane in cyst formation.

The varied presentation of our patients, who had cysts, hematuria, or even an absence of renal anomalies, mirrors the variable renal phenotype seen in mice with *Col4a1* mutations.[6,12,16] Such variability might be explained by the variable location of the identified mutations, with those in exon 25 producing the cystic phenotype. In addition, the role of modifier genes in the ocular phenotype has recently been demonstrated in *Col4a1*$^{+/\Delta ex40}$ mice.[16]

All affected subjects in the three families had the typical retinal arteriolar tortuosity previously reported in both mice and humans.[6,7] However, the systemic angiopathy also affected large vessels, resulting in intracranial aneurysms. A possible factor in the pathophysiological characteristics of intracranial aneurysms is the disruption of the extracellular matrix of the arterial wall.[17,18] Several candidate genes encoding matrix proteins have been identified in linkage studies[19] and analyses of single-nucleotide polymorphisms,[20] but causative genes have not yet been identified, with the exception of *COL3A1* in Ehlers–Danlos syndrome type IV[21] and the polycystic kidney disease 1 gene (*PKD1*).[22] Our results add *COL4A1* to the short list of genes involved in familial intracranial aneurysms.[19]

The p.Gly498→Val and p.Gly528→Glu mutations identified in Families 1 and 3 are associated with muscle cramps. Such cramps might involve transient ischemia or microhemorrhages in the microvasculature or altered skeletal-muscle function linked to defective interaction of mutant COL4A1 with muscle fibers or other matrix components, as observed in Bethlem myopathy (OMIM number 158810).[23,24]

We think that the phenotype may be caused by dominant-negative effects of the mutations, a speculation that is supported by findings from several animal models.[3,6,12,25] Missense mutations of the *COL4A1* and *COL4A2* orthologues in *Caenorhabditis elegans* are associated with a defect in the composition of extracellular-matrix proteins related to the retention of collagen strands in the cytoplasm.[26] Although we found neither retention of the $\alpha1.\alpha1.\alpha2$(IV) trimer in endothelial cells nor a substantial decrease of its expression in the basement membrane, the mutant protein might compete with secretion or integration of the wild-type protein in the basement membrane or might affect the interaction with other basement-membrane components.

In conclusion, *COL4A1* mutations appear to be responsible for a systemic basement-membrane disease. Diagnosis of the HANAC syndrome could be considered in families with unexplained, autosomal dominant hematuria, cystic kidney disease, intracranial aneurysms, and muscle cramps; such consideration would involve funduscopic examination and a search for *COL4A1* mutations.

Supported by grants from INSERM, Université Pierre et Marie Curie, Université Paris Descartes, and Association pour l'Utilisation du Rein Artificiel (AURA). Dr. Van Agtmael is the recipient of a Cardiovascular Research Initiative Wellcome Trust Fellowship.

No potential conflict of interest relevant to this article was reported.

We thank E. Tournier-Lasserve (INSERM Unité 740) for the gift of the *COL4A1–COL4A2* microsatellite markers, M.C. Gubler (INSERM Unité 574) for helpful discussions, C. Combe (Department of Nephrology, University of Bordeaux) for contributions to the clinical evaluation of Family 1, C. Jouanneau and F. Fasani (INSERM Unité Mixte de Recherche Scientifique 702) for technical assistance, and the families for their participation in the study.

REFERENCES

1. Hudson BG, Tryggvason K, Sundaramoorthy M, Neilson EG. Alport's syndrome, Goodpasture's syndrome, and type IV collagen. N Engl J Med 2003;348:2543-56.

2. Miner JH. Developmental biology of glomerular basement membrane components. Curr Opin Nephrol Hypertens 1998; 7:13-9.

3. Gould DB, Phalan FC, Breedveld GJ, et al. Mutations in Col4a1 cause perinatal cerebral hemorrhage and porencephaly. Science 2005;308:1167-71.

4. van der Knaap MS, Smit LM, Barkhof F, et al. Neonatal porencephaly and adult stroke related to mutations in collagen IV A1. Ann Neurol 2006;59:504-11.

5. Breedveld G, de Coo RF, Lequin MH, et al. Novel mutations in three families confirm a major role of COL4A1 in hereditary porencephaly. J Med Genet 2006;43: 490-5.

6. Gould DB, Phalan FC, van Mil SE, et al. Role of COL4A1 in small-vessel disease and hemorrhagic stroke. N Engl J Med 2006;354:1489-96.

7. Vahedi K, Massin P, Guichard JP, et al. Hereditary infantile hemiparesis, retinal arteriolar tortuosity, and leukoencephalopathy. Neurology 2003;60:57-63.

8. Levey AS, Coresh J, Greene T, et al. Using standardized serum creatinine values in the Modification of Diet in Renal Disease Study equation for estimating glomerular filtration rate. Ann Intern Med 2006;145:247-54.

9. Plaisier E, Alamowitch S, Gribouval O, et al. Autosomal-dominant familial hematuria with retinal arteriolar tortuosity and contractures: a novel syndrome. Kidney Int 2005;67:2354-60.

10. Regele HM, Fillipovic E, Langer B, et al. Glomerular expression of dystroglycans is reduced in minimal change nephrosis but not in focal segmental glomerulosclerosis. J Am Soc Nephrol 2000;11:403-12.

11. Ophoff RA, DeYoung J, Service SK, et al. Hereditary vascular retinopathy, cerebroretinal vasculopathy, and hereditary endotheliopathy with retinopathy, nephropathy, and stroke map to a single locus on chromosome 3p21.1-p21.3. Am J Hum Genet 2001;69:447-53.

12. Van Agtmael T, Schlötzer-Schrehardt U, McKie L, et al. Dominant mutations of Col4a1 result in basement membrane defects which lead to anterior segment dysgenesis and glomerulopathy. Hum Mol Genet 2005;14:3161-8.

13. Katz SK, Hakki A, Miller AS, Finkelstein SD. Ultrastructural tubular basement membrane lesions in adult polycystic kidney disease. Ann Clin Lab Sci 1989;19:352-9.

14. Joly D, Morel V, Hummel A, et al. Beta4 integrin and laminin 5 are aberrantly expressed in polycystic kidney disease: role in increased cell adhesion and migration. Am J Pathol 2003;163:1791-800.

15. Shannon MB, Patton BL, Harvey SJ, Miner JH. A hypomorphic mutation in the mouse laminin $\alpha5$ gene causes polycystic kidney disease. J Am Soc Nephrol 2006; 17:1913-22.

16. Gould DB, Marchant JK, Savinova OV, Smith RS, John SW. Col4a1 mutation causes endoplasmic reticulum stress and genetically modifiable ocular dysgenesis. Hum Mol Genet 2007;16:798-807.

17. Chyatte D, Reilly J, Tilson MD. Morphometric analysis of reticular and elastin fibers in the cerebral arteries of patients with intracranial aneurysms. Neurosurgery 1990;26:939-43.

18. Skirgaudas M, Awad IA, Kim J, Rothbart D, Criscuolo G. Expression of angiogenesis factors and selected vascular wall matrix proteins in intracranial saccular aneurysms. Neurosurgery 1996;39:537-45.

19. Ruigrok YM, Rinkel GJ, Wijmenga C. Genetics of intracranial aneurysms. Lancet Neurol 2005;4:179-89.

20. Ruigrok YM, Rinkel GJ, Van't Slot R, Wolfs M, Tang S, Wijmenga C. Evidence in favor of the contribution of genes involved in the maintenance of the extracellular matrix of the artery wall to the development of intracranial aneurysms. Hum Mol Genet 2006;15:3361-8.

21. Pepin M, Schwarze U, Superti-Furga A, Byers PH. Clinical and genetic features of Ehlers–Danlos syndrome type IV, the vascular type. N Engl J Med 2000;342:673-80. [Erratum, N Engl J Med 2001;344:392.]

22. Rossetti S, Chauveau D, Kubly V, et al. Association of mutation position in polycystic kidney disease 1 (PKD1) gene and development of a vascular phenotype. Lancet 2003;361:2196-201.

23. Wiberg C, Hedbom E, Khairullina A, et al. Biglycan and decorin bind close to the n-terminal region of the collagen VI triple helix. J Biol Chem 2001;276:18947-52.

24. Petrini S, Tessa A, Stallcup WB, et al. Altered expression of the MCSP/NG2 chondroitin sulfate proteoglycan in collagen VI deficiency. Mol Cell Neurosci 2005; 30:408-17.

25. Pöschl E, Schlötzer-Schrehardt U, Brachvogel B, Saito K, Ninomiya Y, Mayer U. Collagen IV is essential for basement membrane stability but dispensable for initiation of its assembly during early development. Development 2004;131:1619-28.

26. Gupta MC, Graham PL, Kramer JM. Characterization of alpha1(IV) collagen mutations in Caenorhabditis elegans and the effects of alpha1 and alpha2(IV) mutations on type IV collagen distribution. J Cell Biol 1997;137:1185-96.